PAPER

Check for updates

Effect of noble metals on the performance of Ni–Mo catalysts for the hydrodeoxygenation of lignin oils to fuels

Tove A. Kristensen, [ID] *[ab] Antigoni G. Margellou, [ID] [c] Filip Hallböök,[a] Omar Y. Abdelaziz, [ID] [de] Sara Blomberg, [ID] [a] Christian P. Hulteberg [ID] [ab] and Konstantinos S. Triantafyllidis [ID] [ef]

Improving the catalytic performance in the hydrodeoxygenation (HDO) of lignin oils to produce liquid fuels, while meeting industrial requirements, is important for addressing current environmental challenges. In the present study, the promoting effects of noble metals (Pd, Pt, and Ir) on the performance of the Ni–Mo/CeLa/Al$_2$O$_3$ catalyst were investigated in the HDO of a lignin-derived pyrolysis oil. Catalysts were prepared using incipient wetness impregnation, where 0.5 wt% of the noble metals were impregnated on the catalyst in a final, subsequent step. The HDO experiments were conducted either without or with dimethyl disulfide (DMDS) in a batch reactor at 320 °C and 50 bar (initial H$_2$ pressure at room temperature) for three hours. Interestingly, the highest deoxygenation degree was achieved over the reference catalyst when DMDS was added, in which the resulting oil contained approximately 60% aliphatic and phenolic compounds. Pt showed the most promising promoting effect, which is inferred from its improved hydrogenation capability.

Introduction

The utilization of lignin as a feedstock for liquid fuel production is considered promising and holds significant environmental and socio-economic importance. The advantage of using lignin as a feedstock stems from its classification as a second-generation feedstock and its status as one of the most abundant biopolymers in nature, owing to its role as a major component in lignocellulosic biomass.[1,2] However, due to its structural complexity, it has historically been considered a material with restricted areas of use and is currently mainly utilized for on-site combustion and/or energy recovery.[3,4]

The challenge of using lignin-derived oils (*e.g.*, from pyrolysis) directly as a fuel arises from its poor quality and storage capability. This is mainly caused by the high content of reactive multifunctional oxygenated groups in lignin oils.[4] An upgrading step, in which oxygen is removed, is thus essential before its further use.[5] The hydrodeoxygenation (HDO) of lignin oils is recognized as one of the most promising techniques for overcoming such challenges.[6,7] However, the HDO upgrading process of lignin oils is still facing concerns that need to be considered to improve efficiency and to add industrial value. One of the most critical aspects to emphasize for improving the performance of the HDO upgrading process is the catalyst activity. Catalyst deactivation, due to carbon deposition on the catalyst surface, is one of the most crucial challenges with HDO of lignin-derived oils.[8,9] The compounds in lignin-derived oil comprise bulky phenolic/aromatic dimers and trimers, and have a high affinity for polymerization, which consequently results in carbon deposition on the surface causing blockage of the pores and the active sites.[10]

Great efforts have been made for developing catalysts for the HDO of lignin oils,[7,11-13] and the utilization of noble metals among various catalysts has been recognized as promising for this purpose.[6,12] Noble metals are known for their ability to promote hydrogenation and to enhance the possibility of deep HDO and the removal of the least reactive oxygenated groups.[1,6] An enhanced catalytic hydrogenation capacity is reported to facilitate the dissociation of adsorbed compounds and reduce the risk of polymerization of the resulting carbonium ions.[14] However, despite the demonstrated benefits of using noble metal catalysts in the HDO process, their use is restricted in industry. This is a consequence of the limited metal availability and high costs.[12,15]

aDivision of Chemical Engineering, Department of Process and Life Science Engineering, Lund University, SE-221 00 Lund, Sweden

bHulteberg Chemistry & Engineering AB, SE-212 25 Malmö, Sweden

cDepartment of Chemistry, Aristotle University of Thessaloniki, GR-54124 Thessaloniki, Greece

dDepartment of Chemical Engineering, King Fahd University of Petroleum & Minerals, Dhahran 31261, Saudi Arabia

eInterdisciplinary Research Center for Refining & Advanced Chemicals, King Fahd University of Petroleum & Minerals, Dhahran 31261, Saudi Arabia

fDepartment of Chemistry, King Fahd University of Petroleum & Minerals, Dhahran 31261, Saudi Arabia

Another pronounced disadvantage of using noble metal catalysts in the industrial upgrading process of lignin-derived oils is their sensitivity to deactivation due to sulphur (residue from *e.g.*, the Kraft delignification process).[16] However, the sensitivity for sulphur does not necessarily imply a lack of potential in the HDO process when using noble metals. The use of acidic supports, as for bimetallic catalysts, has been shown to improve the sulphur tolerance of noble metal catalysts and diminish possible poisoning effects.[16,17] For example, Weise *et al.* demonstrated improved activity (up to 46%) of an industrial sulphide Co–Mo/Al$_2$O$_3$ catalyst by the addition of only ppm-level of Pt for the hydrodesulfurization (HDS) process.[18]

In contrast to noble metal catalysts, the Ni–Mo/Al$_2$O$_3$ catalyst is well applied in industrial hydrotreating processes (*e.g.*, HDS). The Ni–Mo/Al$_2$O$_3$ catalyst is also, due to its demonstrated selectivity for HDO and low price, recognized as one of the most commonly used catalysts for the upgrading step of lignin-derived oils.[7,13] In contrast, the Ni–Mo/Al$_2$O$_3$ catalyst needs sulphur to maintain its activity.[19,20]

Considering the above aspects, we herein investigate the promoting effect of adding different noble metals (Pd, Pt, and Ir) to an already enhanced Ni–Mo/Al$_2$O$_3$ catalyst (doped with Ce and La), as previously reported by Kristensen *et al.*,[21] for the HDO process of lignin-derived oils. In general, an increased propensity for direct HDO and reduced carbon deposition were demonstrated for the doped Ni–Mo/Al$_2$O$_3$ catalyst. Different mechanistic aspects over noble metal catalysts and the Ni–Mo/Al$_2$O$_3$ catalysts have been demonstrated for the HDO process, but these studies are primarily focused on model compounds. In contrast, research on validating the catalyst performance using real lignin-derived oil feedstock is limited, yet important for the overall understanding of its industrial prospects. Additionally, the potential promotional value of using the tertiary transition metal system X–Ni–Mo (X being the noble metal) for the HDO of lignin-derived oil is also limited.

In the present study, the improvement of hydrogenation capability is investigated by the addition of Pd, Pt, or Ir onto a Ni–Mo/CeLa/Al$_2$O$_3$ catalyst. The catalyst's activity is evaluated in the HDO process of a lignin-derived oil, both with and without co-feeding a sulphur component, under batch conditions. The performance of the catalysts in this process is also examined in terms of their resistance to short-term deactivation caused by carbon deposition on the catalyst surface, as well as their sensitivity to sulphur poisoning. In addition, the characteristics of the catalysts and their reducibility behaviour are investigated. Finally, the potential of the catalysts for industrial use in the HDO process of lignin-derived oils is assessed.

Experimental

Catalyst synthesis

All metals were impregnated using the incipient wetness method. The reference Ni–Mo/CeLa/Al$_2$O$_3$ catalyst was prepared as previously described by Kristensen *et al.*[21] Overall, 8.0 wt% Mo (ammonium molybdate tetrahydrate, ACS Reagent, Sigma-Aldrich) and 3.5 wt% Ni (nickel(II) nitrate hexahydrate, Sigma-Aldrich) were impregnated on a pretreated doped (using

1 wt% La and 1 wt% Ce) Al$_2$O$_3$ support. Different noble metals, 0.5 wt% of Pd (palladium(II) nitrate solution type ACG, Umicore AG & Co.), Pt (platinum(II) nitrate solution type HNA, Umicore AG & Co.), or Ir (iridium acetate salt, Heraeus), were impregnated onto the Ni–Mo/CeLa/Al$_2$O$_3$ catalyst in a subsequent step. The samples were dried at 120 °C before calcination at 500 °C. Both the set temperatures were reached with a ramp of 2 °C min^{-1} and were held for 4 hours. The catalysts were reduced *ex situ* in H$_2$ (in Ar) at 550 °C for 90 min using a flow rate of 50 cm^3 min^{-1} (STP) prior to being used in the experiments.

Catalyst characterization

The properties of the synthesized catalysts were evaluated using several characterization techniques. Textural properties, metal distribution and crystallinity were examined by N$_2$ physisorption, scanning electron microscopy (SEM), and X-ray diffraction (XRD). The effects of the different noble metals on the catalysts' acidity and reduction behaviour were examined with NH$_3$ chemisorption and Fourier transform-infrared (FT-IR) spectroscopy, and temperature-programmed reduction (TPR), respectively.

N$_2$ physisorption

Determination of N$_2$ adsorption–desorption isotherms for evaluation of the catalysts' textural properties was done using a 3-flex instrument (Micrometrics, Norcross, Georgia, U.S.). A degassing procedure of the samples (approximately 0.5 g) was performed prior to N$_2$ physisorption. This included exposure to temperatures of 90 °C and 250 °C for 30 and 220 min, respectively, using a temperature ramp of 10 °C min^{-1} under vacuum conditions. The Brunauer–Emmett–Teller (BET) equation and the Barrett–Joyner–Halenda (BJH) method were used for determination of the catalysts' specific surface area, and pore volume and pore size, respectively.[22,23] The experimental error of the analysis is ∼5%.

Scanning electron microscopy

High-resolution images of the prepared catalysts were obtained using a field emission scanning electron microscope instrument (JEOL, Akishima, Tokyo, Japan) with an associated field emission gun (X-Max model, Oxford Instruments, Abingdon, UK). Evaluation of the metal distribution throughout the synthesized catalysts was done by performing elemental mapping analysis using an attached energy-dispersive X-ray (EDX) system.

X-ray diffraction

The X-ray powder diffraction (XRD) patterns of the reduced catalysts were recorded with monochromatic CuK$_\alpha$ radiation using a Rigaku Ultima+ 2 cycles X-ray diffractometer. Diffraction was collected for 2 seconds with a step size of 0.02° between 5° and 85°.

NH$_3$ chemisorption

The catalysts' total acidity was determined by static NH$_3$ chemisorption using a 3-flex instrument (Micrometrics, Norcross, Georgia, U.S.). This was done on reduced samples (approximately 0.27 g) at 100 °C. The samples were reduced prior to analysis at 550 °C for 30 min using 10% H$_2$ (in Ar) gas with a flow rate of 10 mL min^{-1}. The temperature set point was reached with a ramp of 10 °C min^{-1}.

Fourier transform-infrared spectroscopy

The characteristics of the acid sites (Brønsted and Lewis acidity) were determined by performing Fourier transform-infrared measurements over the different catalysts with *in situ* adsorption of pyridine (py). A Nicolet 5700 FTIR spectrometer (4 cm^{-2} resolution) with a high-vacuum IR cell (CaF$_2$ cell windows) and OMNIC software was used. The experimental error of the analysis is ~5%. The detailed procedure is described in previous studies.[24,25]

H$_2$ temperature-programmed reduction

Dynamic chemisorption with H$_2$ (10% H$_2$ in Ar) was performed in a 3-flex instrument (Micrometrics, Norcross, Georgia, U.S.) for evaluation of the catalysts' reducibility. The analysis was performed from ambient temperature to 1000 °C under a gas flow of 10 mL min^{-1}. Approximately 0.27 g of each catalyst was evaluated.

HDO activity tests

The lignin-derived oil was produced *via* the fast pyrolysis of commercially available Miscanthus lignin. The HDO activity tests were conducted in a 50 mL stainless-steel high temperature/high pressure batch autoclave reactor (Parr autoclave, model 4848, Moline, IL, the U.S.) at 320 °C for 3 hours under stirring (400 rpm). Approximately 1 g of lignin-derived pyrolysis oil was dissolved in a 20 mL solution of hexadecane/methanol (10 : 1 v% ratio) and added to the reactor together with the catalyst (catalyst-to-feed, C/F = 0.2). Prior to the experiments, the reactor was pressurized and flushed with 50 bar H$_2$ (also used as initial conditions for the experiments) three times to remove air and ensure no leaks. The experiments were conducted either without or with 0.115 mL dimethyl-disulfide (DMDS, used as a sulphur agent). During the hydrotreatment, the pressure at the reaction temperature of 320 °C was 80–84 bar, depending on the type of catalyst and the use or not of DMDS. After the experiment, the reactor was cooled down to ambient temperature whereafter the gaseous products were collected in vacuum bags for further analysis. Vacuum filtration was used to separate the liquid product from the used catalysts. In a subsequent step, ethanol was used to wash the recovered catalysts, multiple times, after which they were dried under vacuum conditions for 6 hours at 80 °C prior to further evaluation.

Product characterization

The gaseous products were analysed *via* a gas chromatograph (GC) equipped with TCD and FID detectors (HP5890 Series II, Agilent Technologies, Santa Clara, CA, USA). The quantification of each gas was based on calibration curves. Regarding the liquid products, they were analysed *via* a gas chromatography-mass spectrometry system (Agilent 6890N-MSD 5973 GC-MS) equipped with an MXT-5 column (Restek, 30 m × 0.25 mm × 0.25 μm). The measurements were performed according to the following heating program: initial temperature 40 °C for 4 min and heating up to 300 °C with heating rate 5 °C min^{-1} and remaining time 7 min. The identification of the compounds was based on the NIST library, and the relative abundance of each compound was calculated as: relative abundance% = 100 × [area of each compound]/[sum of total areas]. Spent catalysts were characterized *via* elemental analysis to evaluate coke depositions. The analysis was performed using the elemental analyser EA 3100 (EuroVector, Pavia, Italy) and the C/H/N/S contents were determined while oxygen content was calculated *via* difference.

Results and discussion

Catalyst characteristics

Table 1 shows an overview of the resulting data from N$_2$-physisorption, NH$_3$-chemisorption and py-FTIR analysis.

The py-FTIR analysis revealed the loss of Brønsted acidity when adding the noble metals. The loss of the Brønsted acidity (Table 1) is suggested to be a result of the interaction between the support and the noble metal species. Al$_2$O$_3$ is recognized to exhibit surface hydroxyl groups with Brønsted acidity characteristics.[26,27] The Brønsted acidity of the reference Ni–Mo catalyst is attributed to the Al$_2$O$_3$ surface hydroxyl groups. Consequently, the hydroxyl groups are recognized to be anchoring sites when impregnating noble metals onto Al$_2$O$_3$.[28,29]

However, the overall results from N$_2$ physisorption and NH$_3$ chemisorption do not imply a significant difference between the

Table 1 Textural and structural properties for the reference (ref) Ni–Mo catalyst and the corresponding catalysts with noble metals (Pd, Pt and Ir, respectively)

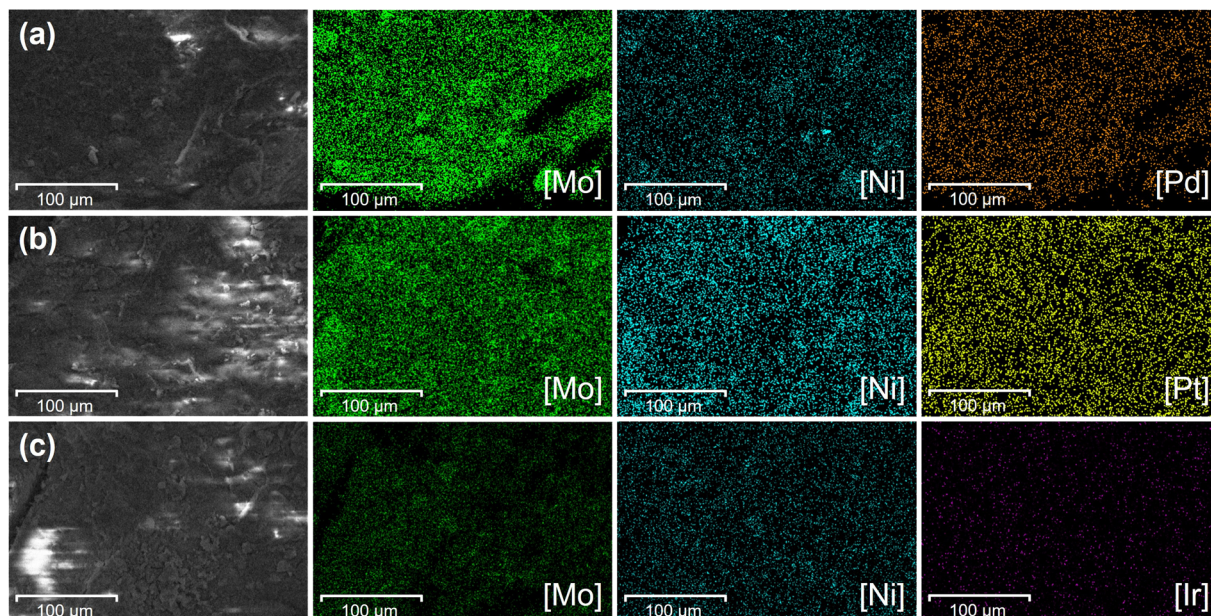| Catalyst	Surface area [m^2 g^{-1}]	Pore diameter [nm]	Pore volume [cm^3 g^{-1}]	Total acidity [cm^3 g^{-1}]	Brønsted acidity [μmol g^{-1}]	Lewis acidity [μmol g^{-1}]	B/L ratio
Ref	59.0	25	0.43	3.16	2.0	57.4	0.035
Pd	52.9	25	0.40	3.33	0	58.3	0
Pt	55.0	25	0.41	3.08	0.5	56.9	0.009
Ir	55.5	26	0.42	3.28	0.1	54.8	0.002

Fig. 1 SEM-EDX images for the elemental mapping of catalysts with (a) Pd, (b) Pt, and (c) Ir.

catalysts related to the textural properties (surface area and pore size) and the total acidity, respectively. Additionally, no diffraction from the noble metals is observed in the XRD patterns (Fig. 2), and the SEM-EDX mapping images (Fig. 1) do not show any metal concentration gradient for the different catalysts, respectively, and an even metal distribution is therefore proposed.

The noble metals also influence the reducibility behaviour of the catalyst. This is interpreted from the resulting TPR profiles shown in Fig. 3. Overall, several hydrogen consumption peaks, assigned to the reducibility behaviour of the alumina supported Ni–Mo catalysts, are observed for all the catalysts.[21,30] In line with similar work reported in the literature, the hydrogen consumption peaks at 480 °C, along with peaks observed between 520 and 640 °C and at 740 °C (Fig. 3), are attributed to the reduction of Mo^{6+} to its metallic form.[21] In particular, the

regimes are assigned to the reduction of Mo^{6+} to Mo^{4+} (dispersed polymeric octahedral species), Mo^{6+} to Mo^{4+} (species with higher degree of polymerization) and Mo^{4+} to metallic, respectively.[31]

However, in our previously reported study, the peak that can be observed at 400 °C (Fig. 3) was proposed to be a result of dispersed surface ceria.[21] Nevertheless, Klimova et al.[31] reported that when promoting the Ni–Mo/γ-Al$_2$O$_3$ catalyst with Pt and Pd, it was observed that reduction of dispersed Mo species (at 370 °C for their reference) did not occur. Instead, higher hydrogen consumption at lower temperatures (217 °C and 260 °C for Pt and Pd, respectively) was observed, which could not be ascribed solely to the presence of noble metals. Klimova et al.[31] proposed, in accordance with other studies, that this could either be due to re-dispersed octahedral Mo^{6+} species as a result of water exposure and the subsequent step of noble metal impregnation, or due to the noble metals (Pt and Pd) facilitating the reduction process.[32,33] Interestingly, similar observations can be identified in our TPR results (Fig. 3). Relative to the reference Ni–Mo
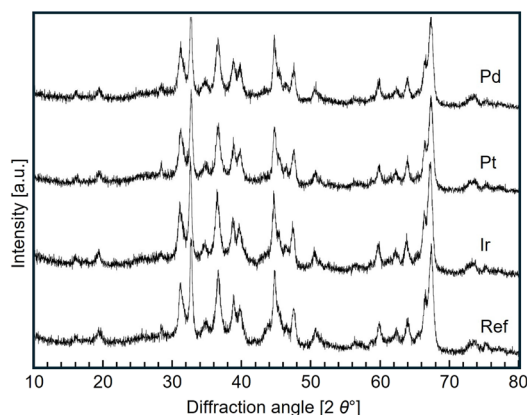

Fig. 2 XRD patterns for the reference Ni–Mo catalyst and the catalysts with Pd, Pt, and Ir, respectively.
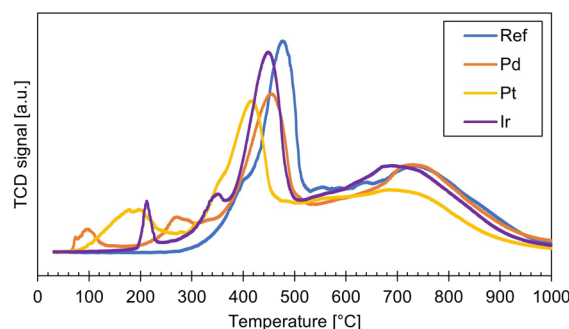

Fig. 3 H_2-TPR profiles of the reference (ref) Ni–Mo catalyst and the catalysts with Pd, Pt, and Ir, respectively.

Sustainable Energy & Fuels

Paper

catalyst, lower hydrogen consumption at approximately 450 °C is observed for the Pd and Pt catalysts (Fig. 3), as well as for the Ir catalyst (Fig. 3). Hence, relatively lower amounts of dispersed Mo^{6+} are suggested to be present in these catalysts. Also, the peak observed at approximately 400 °C for the reference Ni–Mo catalyst is also absent for these catalysts (Pd, Pt and Ir). The peaks at approximately 270 °C and 350 °C for the Pd and Ir catalysts, respectively, are suggested to be the corresponding reduction peaks but are further shifted toward lower temperatures relative to the main peak. The peaks at 100 °C and 210 °C for the Pd and Ir catalysts, respectively, are assigned to the reduction of well-dispersed corresponding noble metal species.[31,34–36] However, in the TPR profile for the Pt catalyst (Fig. 3) only one peak is observed in the lower temperature range (below 450 °C) and is speculated, as reported by Klimova et al.[31], to correspond to a higher hydrogen consumption, which is attributed to reduction of well-dispersed Pt species. It is therefore suggested that the peak observed at 400 °C for the reference Ni–Mo catalyst (Fig. 3) is also attributed to re-dispersed Mo^{6+} species rather than only reduction of ceria as proposed previously, and that the addition of noble metals (Pt, Pd and Ir) facilitates the reduction of octahedral Mo^{6+} species. Additionally, it can be observed that Pt tends to be the most favourable metal for this, as all reduction peaks are shifted towards lower temperatures compared to the reference Ni–Mo catalyst.

Hydrotreatment of lignin-derived oil

The relative abundance of the non-oxygenated compounds of the resulting oils, identified via GC-MS analysis, is presented in Table 2, whereas the liquid and gas compositions are given in Fig. 4 and 5, respectively.

Overall, all catalysts were more active for the HDO process when co-processed with DMDS. Adding DMDS prior to the experiments contributes to higher deoxygenation which led to a lower relative abundance of oxygenated phenols and higher relative abundance of aliphatic compounds in the resulting oils. For the experiments with DMDS, the highest deoxygenation and greatest ratio of aliphatic compounds were achieved over the reference Ni–Mo catalyst, whereas among the noble metal catalysts, the Pt catalyst proved to be the most efficient. Furthermore, the addition of DMDS led to a higher gaseous product yield, which increased from 3.6–4.2 wt% to 12.0–

17.6 wt% (Fig. S1). The increased amount of methane is suggested to be a result of the addition of DMDS. The higher amounts of CO and CO_2 formed when DMDS is used confirmed the higher deoxygenation compared to the experiments without DMDS.

Regarding the composition of hydrotreated bio-oils, all catalysts led to a significant decrease in the relative abundance of oxygenated phenols (OxyPH) from 58% to 15–27% without the addition of DMDS and to 2–10% with DMDS. The reference Ni–Mo catalyst exhibited the highest dealkoxylation activity, while among the noble metals tested, Ir (with DMDS) and Pt were the most efficient. Furthermore, the remaining oxygenated phenols contain one methoxy group (guaiacol (G)-type compounds), which suggests the complete elimination of one methoxy group from the initially present and abundant syringol (S)-type compounds (in initial bio-oil, the ratio of syringol to guaiacol compounds was S/G = 79/21). The dealkoxylation of oxygenated phenols led to an increase in the relative abundance of alkylated phenols (PH). The beneficial effect of DMDS led to a higher concentration of mainly alkyl substituted cycloalkanes with C_5–C_{10} carbon numbers (originating from lignin phenolics), while the rest of the aliphatic compounds are derived from the hydrodeoxygenation of carboxylic acid/esters and the hydrocracking of hexadecane used as the solvent. The esters (EST) identified in the hydrotreated bio-oils are methyl esters, which formation is attributed to the esterification reactions that took place during the hydrotreatment between the carboxylic acid of lignin bio-oil and methanol used as the solvent. Both the addition and the type of noble metal do not lead to remarkable differences among the materials tested.

Various HDO studies using model compounds have been reported and are summarized in numerous reviews.[7,15,37,38] Overall, several competing catalytic hydrotreating reaction routes, including hydrogenation/dehydrogenation, direct deoxygenation, decarboxylation, decarbonylation, and cracking, are recognized over both Ni–Mo catalysts and noble metal-based catalysts, respectively.[6,7,13,14] However, depending on the catalyst composition and whether the metals are in their metallic or sulphided form, different reaction pathways are favoured, and the catalytic activity varies accordingly. For example, as reported by Váchová et al.,[39] catalysts in the metallic state have a higher ability to hydrogenate double bonds and facilitate hydrogenolysis reactions and methanization. This could possibly be the reason for the relatively lower amounts of ethane and C_5/C_6 hydrocarbons in the resulting gas (Fig. 5b and c) over the noble metals compared to the reference Ni–Mo catalyst. Additionally, as reviewed by Cordero-Lanzac et al.,[6] deep HDO is facilitated by an initial hydrogenation step of carbon double bonds, which is proposed to be enhanced by noble metals.

In contrast to these reports, the overall deoxygenation and hydrogenation efficiency of the reference Ni–Mo catalysts observed in the current work was not enhanced with the addition of the noble metals. However, the HDO studies in the literature compare different types of catalysts separately, rather than as tertiary metal-based systems as investigated in this work. However, Klimova et al.[31] and Weise et al.[18] reported

Table 2 The non-oxygenated compounds (expressed as % relative abundance of non-oxygenated compounds identified via GC-MS) of the oils produced after catalytic HDO experiments, comparing cases without and with DMDS addition. The initial lignin pyrolysis bio-oil exhibits 8% relative abundance of non-oxygenated compounds

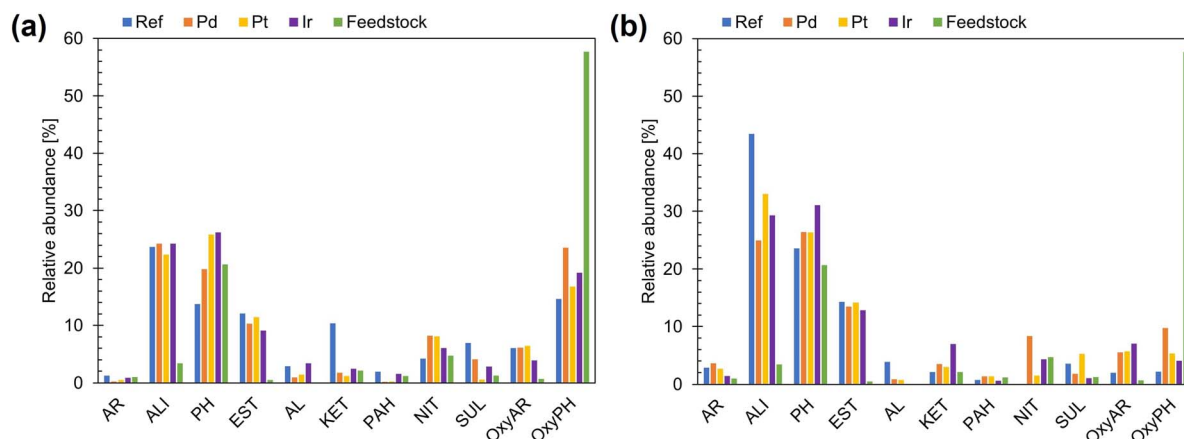| Catalyst	Without DMDS [%]	With DMDS [%]
Ref	28	51
Pd	30	37
Pt	30	44
Ir	30	37

Fig. 4 Classified compounds in the oil after HDO experiments: (a) without DMDS and (b) with DMDS. (AR – aromatics, ALI – aliphatics, PH – alkylated phenols, EST – esters, AL – alcohols, KET – ketones, PAH – polycyclic aromatic hydrocarbons, NIT – nitrogen containing compounds, SUL – sulphur containing compounds, OxyAR – oxygenated aromatics, OxyPH – alkoxylated phenols).
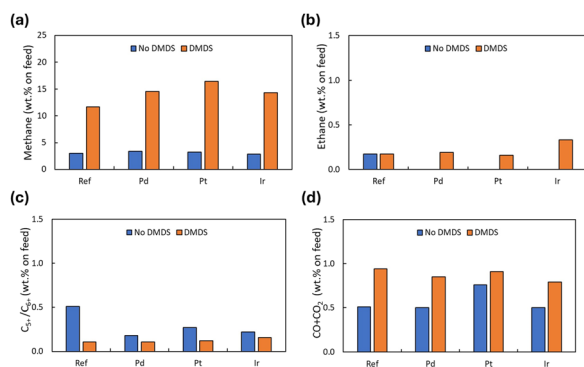

Fig. 5 Gas products resulting from the HDO process, categorized as: (a) methane, (b) ethane, (c) C_5 and C_6, and (d) CO and CO_2.

results indicating enhanced activity over tertiary metal-based Ni–Mo/γ-Al_2O_3 and Co–Mo/γ-Al_2O_3 catalysts, respectively, but in the context of the HDS process. Klimova et al.[31] concluded increased tendencies for initial hydrogenation before hydrodesulfurization of 4,6-DMDBT over Pd or Pt promoted Ni–Mo/γ-Al_2O_3 catalysts. However, no synergistic effect was detected and distinct active phases related to the Ni–Mo co-ordinatively unsaturated sites (CUS) and the noble metal particles were proposed.[31] Weise et al.[18] suggested a catalytic enhancement due to the synergistic atomic effect of Pt on the abundance of CUS in the Mo–Co–S structure, but separate formation of Pt nanoparticles was inferred to saturate the promotional effect. Given this, along with the presumably higher agglomeration propensity of the noble metals investigated herein (significantly higher metal loading per surface area compared to catalysts synthesized by Klimova et al.[31] and Weise et al.[18]), and the acknowledged similarity between the HDS and HDO mechanisms, it is speculated that the active phases are separated into the recognized activation sites of the Ni–Mo catalyst and those of the noble metal-based catalysts investigated herein.

Possible reasons for the absence of increased deoxygenation over the noble metal-based catalysts used herein are therefore speculated to be related to the nature of the noble metals and their restricted ability to activate the compounds, in contrast to the active sites of the Ni–Mo phases. This is because the impact of co-processing with DMDS tends to dominate the resulting deoxygenation rather than the addition of the noble metals. The Mo-sulphide catalysts are more active for the HDO than the corresponding Mo-oxide, and a more prominent effect on the resulting deoxygenation over the different catalysts in the absence of DMDS would otherwise be anticipated. The diminished HDO activity over the noble metal catalysts is speculated to be due to differences in steric hindrance and the increased number of competing reactions, as well as due to differences in noble metal cluster size. For supported noble metal catalysts, the activation of the oxygen-containing compound is proposed to occur either on the metal or at the interface with the support.[12,14]

Lastly, based on the results from the elemental analysis (Fig. 6) of the used catalysts, several overall effects related to the nature of the noble metals and the presence of co-processed DMDS can be observed. Examining the sulphur and oxygen deposition on the used catalyst surfaces, presented in Fig. 6a and b, the most prominent difference is the significantly higher amount of sulphur on the catalyst surface when co-processed with DMDS. This is in accordance with the well-known tendency of Mo catalysts to exist in the sulphide state, forming MoS_2 slabs, rather than the oxidized state.[7,20] However, the impact of the noble metals on the resulting elements on the catalyst surfaces is complex and the reason for the observed differences between the catalysts can be derived from several factors.

Based on the observed differences in sulphur content (Fig. 6a), the noble metals used can form their corresponding metal sulphides, which likely accounts for the higher amounts of sulphur on these catalysts, compared to the reference Ni–Mo catalyst.[18,40,41] The unusually lower amount of sulphur on the catalysts with Ir could be a result of the higher amount of carbon on such catalysts. Another plausible reason for the
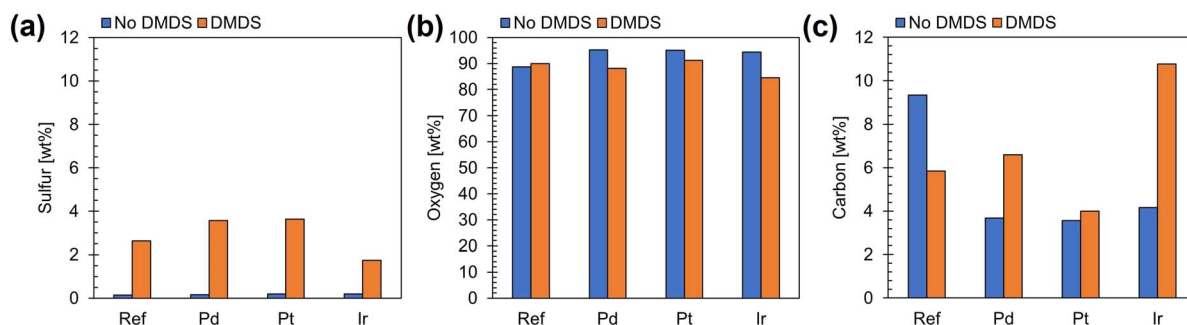
Fig. 6 Elemental analysis of used catalysts showing deposition of (a) sulphur, (b) oxygen, and (c) carbon.

higher amounts of sulphur on the catalysts with noble metals could be inferred from their observed reducibility behaviours (see the TPR profiles in Fig. 3). The TPR profiles revealed that the addition of Pd and Pt facilitates the reduction of Mo^{6+} to Mo^{4+} and could in turn facilitate the formation of MoS_2 slabs. This is in line with work reported by Gulková et al.,[33] who reported increased reducibility of MoS_2 after the addition of Pt. In contrast, the difference in oxygen content on the different catalysts tends to, taking carbon deposition into account, be lower for the catalysts with higher sulphur content.

Finally, examining the carbon deposition on the used catalysts shown in Fig. 6c, both the addition of DMDS and the nature of the noble metal tend to affect the resulting carbon deposition on the corresponding catalysts. However, both acidity and sulphur tolerance affect catalytic activity in the HDO process, which in turn also affects the risk for carbon polymerization. Therefore, the resulting amount of carbon deposition with respect to the relative abundance of non-oxygenated compounds and the acidity of the fresh catalysts are plotted in Fig. 7. The differences in carbon deposition on the catalysts tend to be affected by the nature of the noble metals and their variation in hydrogenation capability. The resulting amount of carbon deposition with respect to the relative abundance of non-oxygenated compounds, presented in Fig. 7, on the used reference Ni–Mo catalyst and the Ir catalyst deviates from a plausible correlation between carbon deposition and acid site concentration. Instead, the results inferred from the data plotted in Fig. 7 suggest differences in hydrogenation capabilities between the metals, as well as in their resistance to sulphur poisoning. From Fig. 7a, less carbon deposition per relative abundance of the non-oxygenated compounds is detected on all the catalysts with a noble metal compared to the reference Ni–Mo catalyst when no DMDS is used. An improvement in catalytic hydrogenation capability reduces the risk of polymerization and in turn implies less carbon deposition on the surface. This is because enhanced hydrogenation more readily saturates the carbonium ions formed during the HDO mechanism with hydrogen, thereby suppressing the polymerization step.[14] However, the improvement in hydrogenation observed upon the addition of the noble metals in the absence of DMDS appears to be reduced for the Pd and Ir catalysts when DMDS is added (Fig. 7b), suggesting a sulphur poisoning effect.

Interestingly, the catalyst with Pt seems to be more resistant to sulphur poisoning in relation to the other noble metals and its hydrogenation capability seems to be preserved. It is speculated that this could be a result of the proposed bimetallic Pt–Mo interactions interpreted from the TPR results (Fig. 3). For example, Yoshimura et al.[42] reported improved tolerance over bimetallic Pd–Pt catalysts, compared to the corresponding monometallic Pd and Pt catalysts. Overall, compared to the other catalysts, in terms of limiting carbon polymerization on the catalyst surface, the Pt catalyst tends to be the best performing catalyst.
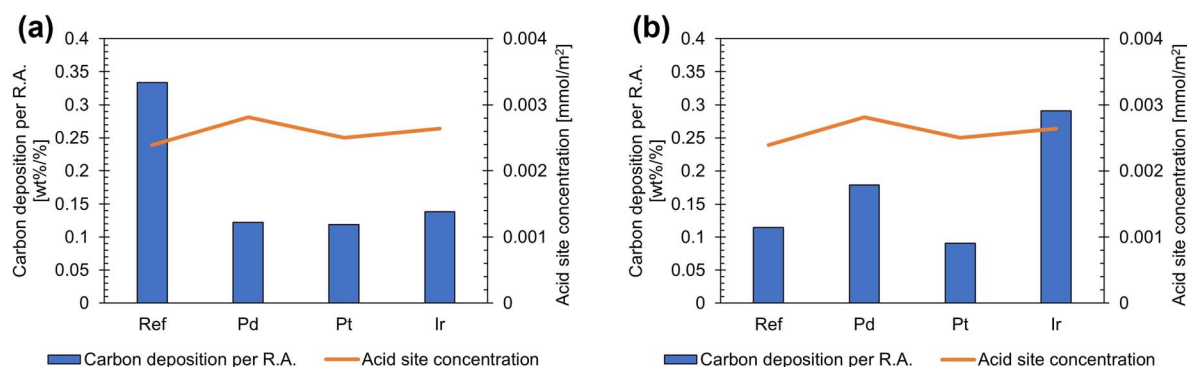

Fig. 7 Carbon deposition on the used catalysts with respect to the relative abundance of non-oxygenated compounds after experiments with (a) no DMDS and (b) DMDS. R.A. is an abbreviation for the relative abundance of non-oxygenated compounds.

Conclusions

The promoting effect of various noble metals (Pd, Pt and Ir) on Ni–Mo/CeLa/Al$_2$O$_3$ catalysts has been investigated for the HDO of a lignin-derived pyrolysis oil. In the prospect of enhancing the industrial value of this process, their resistance to deactivation caused by carbon polymerization and sulphur poisoning was assessed. The HDO experiments implied increased activity for deoxygenation for all the catalysts when co-processed with DMDS. Under these conditions, aliphatic and alkylated-phenolic compounds were predominant with only a few remaining oxygenated phenolics/aromatics. The highest deoxygenation was achieved over the reference Ni–Mo catalyst.

However, lower carbon deposition with respect to the relative abundance of non-oxygenated compounds was observed over the Pt catalyst, which is attributed to its enhanced hydrogenation capability. Work is ongoing, and additional testing for evaluating the potential of using Pt as a promoter in this context is encouraged to enhance prolonged activity compared to the reference Ni–Mo catalyst.

Conflicts of interest

There are no conflicts to declare.

Data availability

Chromatograms and peak areas can be made available upon request.

The main data that support the findings of this study are included within the article and its supplementary information (SI). Supplementary information is available. See DOI: https://doi.org/10.1039/d5se01014d.

Acknowledgements

References

1 M. Zhang, Y. Hu, H. Wang, H. Li, X. Han, Y. Zeng and C. C. Xu, *Mol. Catal.*, 2021, **504**, 111438.

2 R. Patel, P. Dhar, A. Babaei-Ghazvini, M. Nikkhah Dafchahi and B. Acharya, *Bioresour. Technol. Rep.*, 2023, **22**, 101463.

3 O. Y. Abdelaziz, I. Clemmensen, S. Meier, C. A. E. Costa, A. E. Rodrigues, C. P. Hulteberg and A. Riisager, *ChemSusChem*, 2022, **15**, e202201232.

4 J. Gracia-Vitoria, S. C. Gándara, E. Feghali, P. Ortiz, W. Eevers, K. S. Triantafyllidis and K. Vanbroekhoven, *Curr. Opin. Green Sustainable Chem.*, 2023, **40**, 100781.

5 O. Y. Abdelaziz, D. P. Brink, J. Prothmann, K. Ravi, M. Sun, J. García-Hidalgo, M. Sandahl, C. P. Hulteberg, C. Turner, G. Lidén and M. F. Gorwa-Grauslund, *Biotechnol. Adv.*, 2016, **34**, 1318–1346.

6 T. Cordero-Lanzac, J. Rodríguez-Mirasol, T. Cordero and J. Bilbao, *Energy Fuels*, 2021, **35**, 17008–17031.

7 Y. W. Cheah, M. A. Salam, J. Sebastian, S. Ghosh, P. Arora, O. Öhrman, L. Olsson and D. Creaser, *J. Environ. Chem. Eng.*, 2023, **11**, 109614.

8 T. Cordero-Lanzac, R. Palos, I. Hita, J. M. Arandes, J. Rodríguez-Mirasol, T. Cordero, J. Bilbao and P. Castaño, *Appl. Catal., B*, 2018, **239**, 513–524.

9 T. Kristensen, C. Hulteberg, S. Blomberg, P. Tunå and O. Abdelaziz, *Top. Catal.*, 2023, **66**, 1341–1352.

10 H. Wang and Y. Wang, *Top. Catal.*, 2016, **59**, 65–72.

11 M. M. Ambursa, J. C. Juan, Y. Yahaya, Y. H. Taufiq-Yap, Y. C. Lin and H. V. Lee, *Renewable Sustainable Energy Rev.*, 2021, **138**, 110667.

12 S. Alkhoori, M. Khaleel, L. F. Vega and K. Polychronopoulou, *J. Ind. Eng. Chem.*, 2023, **127**, 36–61.

13 A. S. Ouedraogo and P. R. Bhoi, *J. Cleaner Prod.*, 2020, **253**, 119957.

14 P. M. Mortensen, J. D. Grunwaldt, P. A. Jensen, K. G. Knudsen and A. D. Jensen, *Appl. Catal., A*, 2011, **407**, 1–19.

15 A. Gil, I. Sancho-Sanz and S. A. Korili, *Ind. Eng. Chem. Res.*, 2024, **63**, 11759–11775.

16 K. Yang, X. Chen, Z. Bai and C. Liang, *Catal. Today*, 2021, **377**, 205–212.

17 K. J. Kim, Y. L. Lee, G. R. Hong, S. Y. Ahn, B. J. Kim, S. S. Lee, Y. Jeon and H. S. Roh, *Catal. Today*, 2024, **425**, 114361.

18 C. F. Weise, H. Falsig, P. G. Moses, S. Helveg, M. Brorson and L. P. Hansen, *J. Catal.*, 2021, **403**, 74–86.

19 H. Ojagh, D. Creaser, S. Tamm, P. Arora, S. Nyströ, E. Lind Grennfelt and L. Olsson, *Ind. Eng. Chem. Res.*, 2017, **56**, 5547–5557.

20 P. M. Mortensen, D. Gardini, C. D. Damsgaard, J. D. Grunwaldt, P. A. Jensen, J. B. Wagner and A. D. Jensen, *Appl. Catal., A*, 2016, **523**, 159–170.

21 T. A. Kristensen, C. P. Hulteberg, R. L. Wallenberg, O. Y. Abdelaziz and S. Blomberg, *Energy Fuels*, 2024, **38**, 9827–9835.

22 S. Brunauer, P. H. Emmett and E. Teller, *J. Am. Chem. Soc.*, 1938, **60**, 309–319.

23 E. P. Barrett, L. G. Joyner and P. P. Halenda, *J. Am. Chem. Soc.*, 1951, **73**, 373–380.

24 A. G. Margellou, F. F. Zormpa, D. Karfaridis, S. A. Karakoulia and K. S. Triantafyllidis, *Catalysts*, 2025, **15**, 48.

25 F. F. Zormpa, A. G. Margellou, S. A. Karakoulia, E. Delli and K. S. Triantafyllidis, *Catal. Today*, 2024, **433**, 114654.

26 Z. Wang, Y. Jiang, O. Lafon, J. Trébosc, K. D. Kim, C. Stampfl, A. Baiker, J.-P. Amoureux and J. Huang, *Nat. Commun.*, 2016, **7**, 13820.

27 M. Zaki, F. Al-Sagheer, H. Khalaf, M. I. Zaki, M. A. Hasan, F. A. Al-Sagheer and L. Pasupulety, *Colloids Surf., A*, 2001, **190**, 261–274.

28 Z. Zhang, G. He, Y. Li, C. Zhang, J. Ma and H. He, *Environ. Sci. Technol.*, 2022, **56**, 10916–10924.

29 Y. Choi, G. Kim, J. Kim, S. Lee, J. C. Kim, R. Ryoo and H. Lee, *Appl. Catal., B*, 2023, **325**, 122325.

30 S. Blomberg, N. Johansson, E. Kokkonen, J. Rissler, L. Kollberg, C. Preger, S. M. Franzén, M. E. Messing and C. Hulteberg, *Materials*, 2019, **12**, 3727.

31 T. Klimova, P. M. Vara and I. P. Lee, *Catal. Today*, 2010, **150**, 171–178.

32 R. López Cordero and A. López Agudo, *Appl. Catal., A*, 2000, **202**, 23–35.

33 D. Gulková, Y. Yoshimura and Z. Vít, *Appl. Catal., B*, 2009, **87**, 171–180.

34 A. Tanksale, J. N. Beltramini, J. A. Dumesic and G. Q. Lu, *J. Catal.*, 2008, **258**, 366–377.

35 M. Zieliński, M. Kot, M. Pietrowski, R. Wojcieszak, J. Kowalska-Kuś and E. Janiszewska, *Materials*, 2021, **14**, 4465.

36 B. Pawelec, C. V. Loricera, C. Geantet, N. Mota, J. L. G. Fierro and R. M. Navarro, *Mol. Catal.*, 2020, **482**, 110669.

37 P. Lahijani, M. Mohammadi, A. R. Mohamed, F. Ismail, K. T. Lee and G. Amini, *Energy Convers. Manage.:X*, 2022, **268**, 115956.

38 A. L. Jongerius, R. Jastrzebski, P. C. A. Bruijnincx and B. M. Weckhuysen, *J. Catal.*, 2012, **285**, 315–323.

39 V. Váchová, D. Toullis, P. Straka, P. Šimáček, M. Staš, A. Gdovin, Z. Beňo and J. Blažek, *Energy Fuels*, 2020, **34**, 9609–9619.

40 M. González-Ildelfonso, J. Escobar, E. Gordillo-Cruz, P. del Ángel, V. A. Suárez-Toriello and J. A. De los Reyes, *Mater. Chem. Phys.*, 2022, **278**, 125568.

41 J. Cinibulk, D. Gulková, Y. Yoshimura and Z. Vít, *Appl. Catal., A*, 2003, **255**, 321–329.

42 Y. Yoshimura, M. Toba, T. Matsui, M. Harada, Y. Ichihashi, K. K. Bando, H. Yasuda, H. Ishihara, Y. Morita and T. Kameoka, *Appl. Catal., A*, 2007, **322**, 152–171.